Biocompatible and totally disintegrable semiconducting polymer for ultrathin and ultralightweight transient electronics

Ting Lei[a], Ming Guan[b], Jia Liu[a], Hung-Cheng Lin[a], Raphael Pfattner[a], Leo Shaw[a], Allister F. McGuire[c], Tsung-Ching Huang[d], Leilai Shao[e], Kwang-Ting Cheng[e], Jeffrey B.-H. Tok[a], and Zhenan Bao[a,1]

[a]Department of Chemical Engineering, Stanford University, Stanford, CA 94305; [b]Department of Materials Science and Engineering, Stanford University, Stanford, CA 94305; [c]Department of Chemistry, Stanford University, Stanford, CA 94305; [d]Hewlett Packard Labs, Palo Alto, CA 94304; and [e]Department of Electrical and Computer Engineering, University of California, Santa Barbara, CA 93106

Edited by John A. Rogers, University of Illinois, Urbana, IL, and approved April 4, 2017 (received for review January 26, 2017)

Increasing performance demands and shorter use lifetimes of consumer electronics have resulted in the rapid growth of electronic waste. Currently, consumer electronics are typically made with nondecomposable, nonbiocompatible, and sometimes even toxic materials, leading to serious ecological challenges worldwide. Here, we report an example of totally disintegrable and biocompatible semiconducting polymers for thin-film transistors. The polymer consists of reversible imine bonds and building blocks that can be easily decomposed under mild acidic conditions. In addition, an ultrathin (800-nm) biodegradable cellulose substrate with high chemical and thermal stability is developed. Coupled with iron electrodes, we have successfully fabricated fully disintegrable and biocompatible polymer transistors. Furthermore, disintegrable and biocompatible pseudo-complementary metal–oxide–semiconductor (CMOS) flexible circuits are demonstrated. These flexible circuits are ultrathin (<1 μm) and ultralightweight (~2 g/m^2) with low operating voltage (4 V), yielding potential applications of these disintegrable semiconducting polymers in low-cost, biocompatible, and ultralightweight transient electronics.

organic electronics | flexible electronics | conjugated polymers | thin-film transistors | biodegradable materials

Current consumer electronic devices are usually made with nondecomposable and often toxic inorganic semiconductors that typically require high-vacuum and high-temperature manufacturing processes. With rapid technological advancement and short turnovers for electronic devices, the colossal demand for electronics has led to a huge amount of waste and rapid consumption of scarce elements like gallium and indium. For example, indium gallium zinc oxide (IGZO) has been widely used in many thin-film transistor (TFT) applications, such as active-matrix organic light emitting diode backplanes, radio frequency identification tags, electronic paper, and sensor devices (1). The growing trend for devices comprising the so-called "Internet of Things" (IoT) will involve an even larger number of electronics, likely straining our existing natural resource supplies and imposing an even greater influence on our precious and fragile environment. To address these issues, transient electronics, or "green" electronics, have emerged as a new class of technologies whose key feature is that they physically "disappear" after being used and/or disposed (2–5). Aside from the environmental benefits, transient electronics also open up a new application space, such as (i) implantable medical devices that are resorbable by the human body, thus bypassing the need for surgery to extract them and (ii) secure electronics that can totally disintegrate in a controlled fashion, thus rendering them untraceable. In pursuit of these goals, silicon-based transient electronics have recently been reported (2, 3), and are able to degrade under mild base. However, devices based on inorganic materials such as silicon are mechanically brittle and require high-vacuum, high-temperature, and generally high-cost manufacturing processes. Compared with their inorganic counterparts, organic semiconductors are made of abundant carbon-based components. Organic electronics can be synthesized and processed with low-temperature and, more importantly, have the potential to be environmentally benign candidates for electronic applications (4). Organic semiconductors have been widely used in chemical and biological sensors (6), health monitors (7), stretchable devices (8), and electronic skin (9). To date, most studies on organic semiconductors have focused on material synthesis and device fabrication with little emphasis on their environmental impact and biocompatibility (10, 11). Although some biodegradable small molecules, e.g., β-carotene and indigo derivatives, have been investigated (12, 13), these small-molecule semiconductors have either low carrier mobilities (<0.1 cm^2/Vs) or require high-vacuum deposition processes.

Conjugated polymers can be mechanically flexible, stretchable, and solution-processable at low temperatures, making them amenable to the low-cost production of flexible and stretchable electronics using roll-to-roll manufacture (14). The recent development of donor−acceptor (D−A) polymers has greatly improved the device performance, with field-effect transistor (FET) mobilities surpassing that of amorphous silicon (0.1−1 cm^2/Vs) and with solar cell efficiencies beyond 10% (15, 16). Conjugated polymers have emerged as one of the most promising candidates for flexible TFTs. Compared with nonconjugated decomposable polymers, molecular design choices for conjugated decomposable polymers are highly limited because there are only a few decomposable

Significance

Organic electronics, particularly polymers, can be synthesized and processed with low temperatures and, more importantly, have the potential to be environmentally benign candidates for electronic applications. However, there has been no report of totally decomposable polymer semiconductors. Their availability will enable low-cost and fully disintegrable transient electronics. We have developed an innovative concept based on imine chemistry that allows totally disintegrable and biocompatible semiconducting polymers. Using an ultrathin biodegradable substrate, we successfully fabricated polymer transistors and logic circuits that show high performance and are ultralightweight, but they can be fully disintegrable. Our work significantly advances organic materials to enable environmentally friendly and biointegrated electronic applications.

Author contributions: T.L. and Z.B. designed research; T.L., M.G., J.L., H.-C.L., R.P., L. Shaw, A.F.M., T.-C.H., L. Shao, and K.-T.C. performed research; T.L. contributed new reagents/analytic tools; T.L., L. Shaw, and Z.B. analyzed data; and T.L., J.B.-H.T., and Z.B. wrote the paper.

The authors declare no conflict of interest.

This article is a PNAS Direct Submission.

[1]To whom correspondence should be sent. Email: zbao@stanford.edu.

This article contains supporting information online at www.pnas.org/lookup/suppl/doi:10.1073/pnas.1701478114/-/DCSupplemental.

molecular building blocks available. To our knowledge, there have not yet been any reports of totally decomposable conjugated polymers or polymer-based electronics.

To realize "green" electronics with zero footprint, an ideal approach is using semiconducting polymers that can be synthesized from natural resources and decomposed back to the environment (Fig. 1*A*). In this work, we demonstrate several key steps of the "ideal cycle" in Fig. 1*A* by using imine bonds as the reversible conjugated linker to illustrate an example of a totally-disintegrable conjugated polymer and its application in organic electronics. Ultrathin electronics provide ultra-lightweight, extreme flexibility, and better conformability, which are important for imperceptible electronics (7), conformal biological sensors (17), and stretchable devices (18). While ultrathin and lightweight organic flexible devices on plastic substrates, e.g., polyethylene terephthalate (PET), have been previously developed (7, 18, 19), we report here a type of biodegradable ultrathin (800 nm) substrate based on cellulose for ultra-lightweight (2 g/m^2) electronics (Fig. 1*B*). Our substrate is highly compatible with electronics fabrication processes due to its stability in a variety of commonly-used organic and aqueous solutions, along with its high temperature stability (glass transition temperature (T_g) >180 °C). Using these materials, we proceeded to fabricate ultrathin flexible pseudo-complementary metal–oxide–semiconductor (CMOS) circuits with high gain and rail-to-rail output voltage swings at a low operation voltage of 4 V. With iron electrodes, fully disintegrable transient devices are demonstrated, in which we observed these devices' complete disintegration after 30 d upon exposure to mildly acidic conditions.

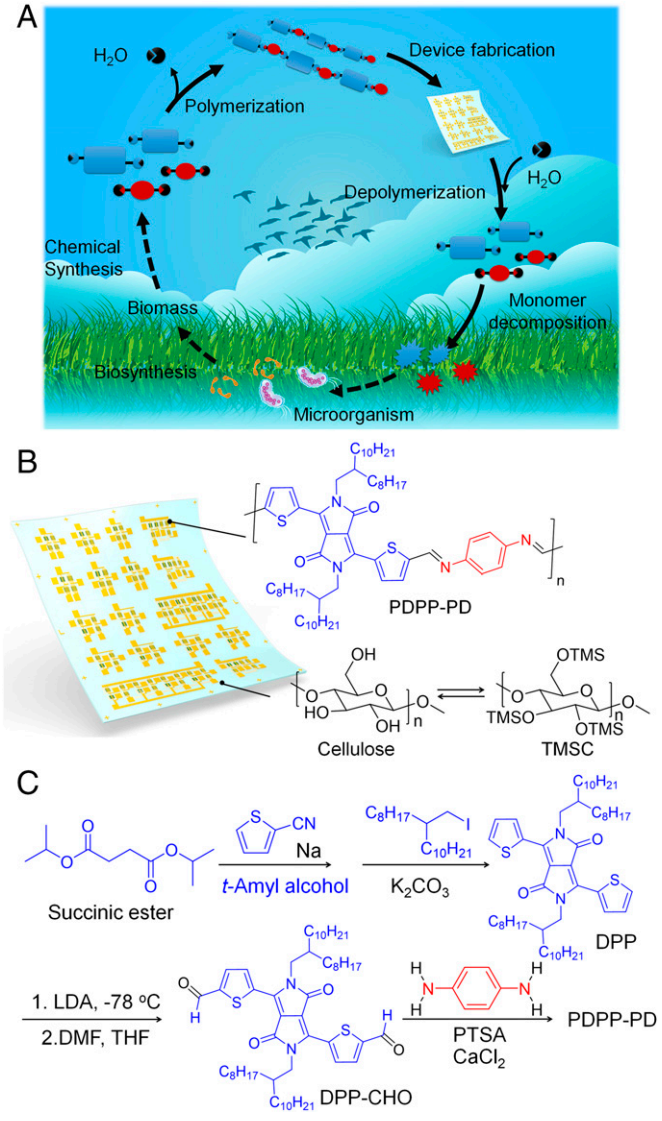

Fig. 1. Schematics of polymer-based transient "green" electronics. (*A*) Polymer synthesis, fabrication, and decomposition cycle for transient polymer electronics. Solid lines indicate the processes demonstrated in this paper. Dashed lines are the envisioned processes that might be realized in the future. (*B*) Flexible device using disintegrable polymers as the active material or substrate. *Inset* shows the fabrication of the cellulose substrate using a reversible functionalization chemistry. (*C*) Synthesis of the disintegrable PDPP-PD using imine chemistry.

Decomposable Polymer Design and Characterization

Dyes synthesized from natural resources, such as isoindigo or diketopyrrolopyrrole (DPP), are incorporated into conjugated polymers as they are important molecular building blocks to impart high charge carrier mobilities (15, 16). DPP is selected because it can be easily functionalized chemically, and, more importantly, we observed that the DPP monomer can be degraded further (see below). The imine bond (–C=N–) is a stable conjugated linker under neutral-pH conditions (20), but it can be readily hydrolyzed with a catalytic amount of acid (21). Although imine bonds have been used as building blocks for conjugated polymers and covalent organic frameworks (22, 23), they have not been explored in the design of decomposable conjugated polymers and totally disintegrable electronics. Fig. 1*C* shows the synthetic procedure for the decomposable polymer PDPP-PD. DPP can be synthesized in two steps: (*i*) react succinic ester and 2-thiophenecarbonitrile in *tert*-amyl alcohol; (*ii*) attach branched alkyl chains to increase the solubility. The branched alkyl chain was synthesized from octyldodecanol. Among these chemicals, succinic ester and *tert*-amyl alcohol can be obtained from natural resources, and octyldodecanol is a nontoxic ingredient widely used in a variety of beauty products. Two aldehyde groups were introduced to the DPP monomer, giving DPP-CHO in 77% yield. PDPP-PD was synthesized through a condensation reaction between DPP-CHO and *p*-phenylenediamine under catalysis with *p*-toluenesulfonic acid (PTSA). We initially prepared the polymer in the absence of any drying agent, and the polymer obtained exhibited a low weight-averaged molecular weight (M_w) of 19.1 kDa. After adding $CaCl_2$ as a drying agent, we are able to obtain a higher M_r of 39.6 kDa. Removal of reaction-generated water obviously increased the polymer's molecular weight. Notably, imine polymerization does not require any noble metal catalysts or toxic phosphorous ligands that are typically used for traditional conjugated polymer synthesis. In this way, the synthesis of imine polymers is more economical and environmentally friendly. The decomposable polymer is stable under ambient conditions and was observed to have a decomposition temperature above 400 °C (*SI Appendix*, Fig. S1). The highest occupied molecular orbital (HOMO) and lowest unoccupied molecular orbital (LUMO) of the polymer measured by cyclic voltammetry are –5.11 and –3.54 eV, respectively. These values agreed well with our predictions as calculated by density functional theory (*SI Appendix*, Fig. S2).

Fig. 2*A* shows the absorption spectrum and color changes of PDPP-PD after adding 1% (vol/vol) acetic acid in water. The main absorption peak (680 nm) decreased significantly after 3 h and completely disappeared after 10 d. Moreover, the solution color was observed to change from blue to purple during this duration. After a 10-d decomposition test, the absorption spectrum and solution color were both similar to that of the pure monomer DPP-CHO. After a 40-d test, the purple color was observed to disappear completely to become a clear solution, indicating the polymer was totally disintegrated under acidic conditions. The polymer decomposition can occur in good solvents (e.g., chloroform), in poor solvents (e.g., THF; *SI Appendix*, Fig. S3), and in the thin film. The "good" solvents have a stronger ability to solvate

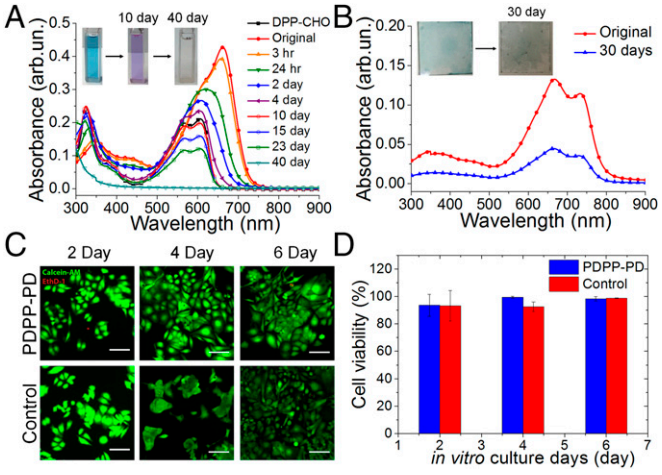

Fig. 2. Degradability and biocompatibility of PDPP-PD. (*A*) Absorption spectrum changes in PDPP-PD's decomposition process. (*Inset*) Photos of polymer solution color changes after decomposition for 10 d and for 40 d. (*B*) Absorption spectrum changes for a polymer film before and after decomposition in a pH 4.6 buffer solution. (*Inset*) Photos of the film before and after decomposition. (*C*) Fluorescent images of live HL-1 cardiomyocytes stained with calcein-AM (green) and EthD-1 (red). (Scale bar: 100 μm.) (*D*) Viability of HL-1 cardiomyocytes on 2, 4, and 6 d of in vitro culture (n > 1,000 cells for each data bar).

the polymer and facilitate the separation into individual chains. On the contrary, for the "poor" solvent, the polymer tends to aggregate in solution. As shown in Fig. 2*B*, after soaking the spin-coated polymer film (40 nm) in a pH 4.6 aqueous buffer solution, the polymer thin-film absorption decreased steadily over time, indicating its degradation. These results suggest that the polymer can be decomposed not only in solution (either as free polymer or as aggregates) but also in solid state. In contrast, the polymer is stable under neutral and basic conditions, as we did not observe noticeable decomposition of the polymer in solution (*SI Appendix*, Fig. S4). Based on the absorption spectra and in situ NMR studies (*SI Appendix*, Figs. S5 and S6), we propose that the polymer decomposition proceeds in two steps (*SI Appendix*, Fig. S7): (*i*) the imine bonds are hydrolyzed under acid catalysis and (*ii*) water further decomposes the DPP monomers through the hydrolysis of the lactam rings. In the first step, we observed clear NMR signatures of the DPP-CHO and phenylenediamine monomers, consistent with polymer decomposition. In the second step, the lactam ring hydrolyzation is supported by the absorption spectrum, where the purple-colored DPP-CHO became colorless after decomposition.

Biocompatibility is a highly desirable requirement for implantable medical devices or sensory devices that directly interface with living tissue (4). Semiconducting polymers with good biocompatibility enable the development of organic FET devices for biosensors and prosthetic skins (24). To prove the biocompatibility of PDPP-PD, we performed in vitro cell culture experiments using our polymer coated on a glass slide as the substrate (Fig. 2 *C* and *D*). HL-1 cardiomyocytes were used for biocompatibility test, because HL-1 cell is a standard cell line for electrophysiological testing. We can potentially use the fabricated electronics to detect the electrophysiological signals (25). Our cell viability measurements showed that the PDPP-PD has negligible effect on the viability of HL-1 cardiomyocytes from 2 to 6 d at pH 7.4.

Ultrathin Cellulose Substrate for TFTs

To realize ultrathin transient electronics, substrates that are tough, compatible with mild processing conditions, and biodegradable are needed. In addition, the substrate should have high temperature stability to allow for the thermal annealing of the semiconducting and dielectric layers. Because organic solvents are used during the spin-coating of the polymer films and a water-aided peel-off process is used during fabrication (26), good chemical and water stability are also needed. Other reported biodegradable substrates, such as silk (3) or poly(lactide-coglycolide) (PLGA) (5, 27), are either not resistant to water or organic solvent, or are not heat tolerant. We realized that regenerated cellulose films (RCFs) are a good candidate because of their high thermal stability [decomposition temperature (T_d) > 210 °C, T_g > 180 °C], high transparency, good flexibility, and biodegradability (28, 29). Moreover, cellulose films have been previously used as biodegradable substrates in electronics (28–30). However, these cellulose films are typically made with thicknesses well over 10 μm and thus cannot be used to fabricate ultrathin electronics with substrate thicknesses below 1–2 μm (7, 18, 19). To the best of our knowledge, there have been no reports on ultrathin (1–2 μm) biodegradable substrates for electronics. Thus, to realize them, we subsequently developed a method described herein to obtain ultrathin (800 nm) cellulose films (Fig. 1*B* and *SI Appendix*, Fig. S8). First, microcrystalline cellulose powders were dissolved in LiCl/*N*,*N*-dimethylacetamide (DMAc) and reacted with hexamethyldisilazane (HMDS) (31, 32), providing trimethylsilyl-functionalized cellulose (TMSC) (Fig. 1*B*). To fabricate films or devices, TMSC in chlorobenzene (CB) (70 mg/mL) was spin-coated on a thin dextran sacrificial layer. The TMSC film was measured to be 1.2 μm. After hydrolyzing the film in 95% acetic acid vapor for 2 h, the trimethylsilyl groups were removed, giving a 400-nm-thick cellulose film. The film thickness significantly

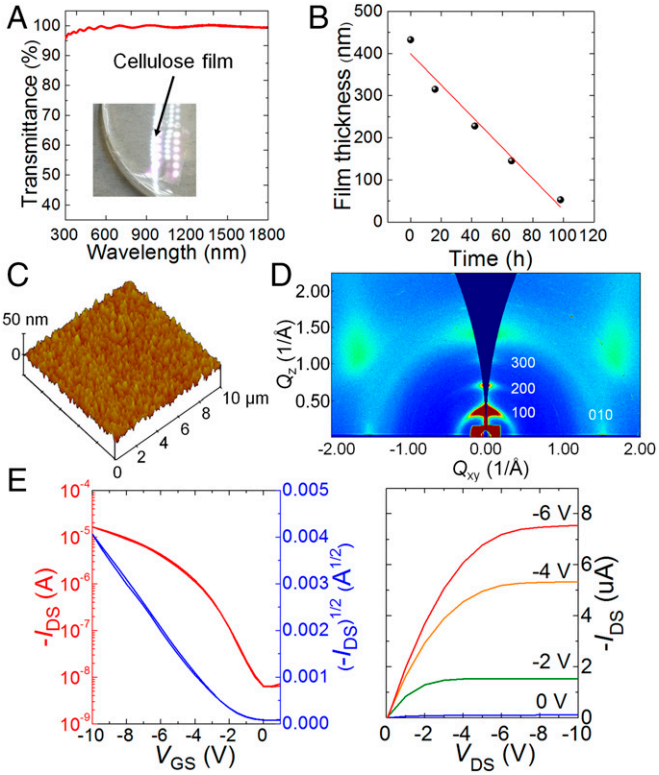

Fig. 3. Characterization of the ultrathin cellulose film and PDPP-PD polymer transistor. (*A*) Optical transmittance of an 800-nm-thick cellulose film. (*Inset*) Photo of a cellulose film floating on water. (*B*) Film thickness changes of a cellulose film soaked in a 1 mg/mL cellulase buffer solution (cellulase from *Trichoderma viride*; pH 4.6). The film shows a linear decomposition speed of 3.7 nm/h. (*C*) AFM height image of a cellulose film. (*D*) 2D-GIXD image of the polymer film (color scale is linear). (*E*) Transfer and output characteristics of PDPP-PD fabricated on a 800-nm cellulose substrate (50-nm Al_2O_3, V_{DS} = −10 V).

decreased to one-third of the original film thickness, largely due to the removal of the bulky trimethylsilyl groups. The hydrolyzed cellulose film is insoluble in most organic solvents, for example, toluene, THF, chloroform, CB, and water. Thus, we can sequentially repeat the above steps to obtain an 800-nm-thick film, which is robust enough for further device fabrication and peel-off. By soaking the device in water, the dextran layer is dissolved, starting from the edges of the device to the center. This process ultimately releases the ultrathin substrate and leaves it floating on water surface (Fig. 3*A*, *Inset*).

For optoelectronic applications, high optical transparency is desirable. The optical properties of the cellulose film were characterized with UV-vis spectroscopy. The 800-nm-thick film exhibited a high transmittance of 99.7% at 550 nm (Fig. 3*A*) and >98% from 400 to 1,800 nm. The surface rms roughness characterized by atomic force microscopy (AFM) is 3.9 nm (Fig. 3*C*), smaller than other RCFs (6–7 nm) and commercial PET films (7.0 nm) (30). Low surface roughness allows for electronics to be fabricated directly on the film and also provides higher device yields and performance. The cellulose film is stable in organic solvents and neutral aqueous media, but can be easily disintegrated by cellulase in mild acid conditions. The degradability of the cellulose film was monitored by soaking the cellulose film in a 1 mg/mL cellulase (from *Trichoderma viride*) buffer solution (pH 4.6) (Fig. 3*B*). The film degraded at a constant rate about 3.7 nm/h. Under these conditions, an 800-nm-thick cellulose film completely disintegrated after 10 d.

The electrical performance of PDPP-PD was first evaluated by spin-coating 5 mg/mL polymer solutions on octadecyltrimethoxysilane (OTS)-treated SiO_2 (300 nm)/n^{++}-Si substrates. The bottom-gate/top-contact device configuration was used with gold for the source-drain electrodes. For low–molecular-weight PDPP-PD (M_r = 19.1 kDa), the polymer exhibited low hole mobilities of 0.042 ± 0.006 cm^2/V·s. In contrast, higher molecular-weight PDPP-PD (M_r = 39.6 kDa) demonstrated hole mobilities of 0.34 ± 0.04 cm^2/V·s (*SI Appendix*, Figs. S9 and S10), nearly one order of magnitude higher than the former. Unlike many high-mobility conjugated polymers that show kinked transfer characteristics (33), PDPP-PD exhibited nearly ideal transfer characteristics. The device performance on the 800-nm cellulose film with atomic layer deposition (ALD) deposited Al_2O_3 as the dielectric layer is shown in Fig. 3*E*. The device possessed hole mobilities of 0.21 ± 0.03 cm^2/V·s with good on/off ratios (*SI Appendix*, Fig. S11). Because of the low-lying HOMO level of PDPP-PD, the device is water- and air-stable even without any encapsulation. To analyze the polymer film microstructure, grazing-incidence X-ray diffraction (GIXD) was performed (Fig. 3*D* and *SI Appendix*, Fig. S12). Distinct out-of-plane peaks from the (*h*00) reflections can be seen up to third order with a weak fourth-order peak convolved with a halo of diffuse alkyl scattering and π-stacking diffraction. The crystalline lamella have a Q(100) value of 0.36 $Å^{-1}$, which is equivalent to a d-spacing of 17.5 Å. The (010) peak occurs at 1.51 $Å^{-1}$, which corresponds to a π-stacking distance of 4.16 Å, a distance slightly larger than typical for most semiconducting polymers (~3.6–3.9 Å) (15), possibly due to a less-planar polymer backbone (*SI Appendix*, Fig. S13). Both edge-on and face-on packing are found in the thin film, which has previously been shown to be beneficial for charge transport (34).

Solution-Processed Disintegrable Pseudo-CMOS Circuits

To demonstrate the potential of our decomposable polymer semiconductor and substrate, we proceed to fabricate pseudo-CMOS logic circuits (Figs. 1*B* and 4*A*). Such circuits use only one type of semiconductor but have performance comparable to complementary-type logic circuits, which significantly reduces the fabrication complexity (35). Based on this design, high-performance organic small-molecule and metal oxide flexible circuits have been demonstrated (36, 37). The good chemical and thermal stability of the cellulose substrate allow for direct device fabrication on top. Gold was used as the gate, source, drain, and

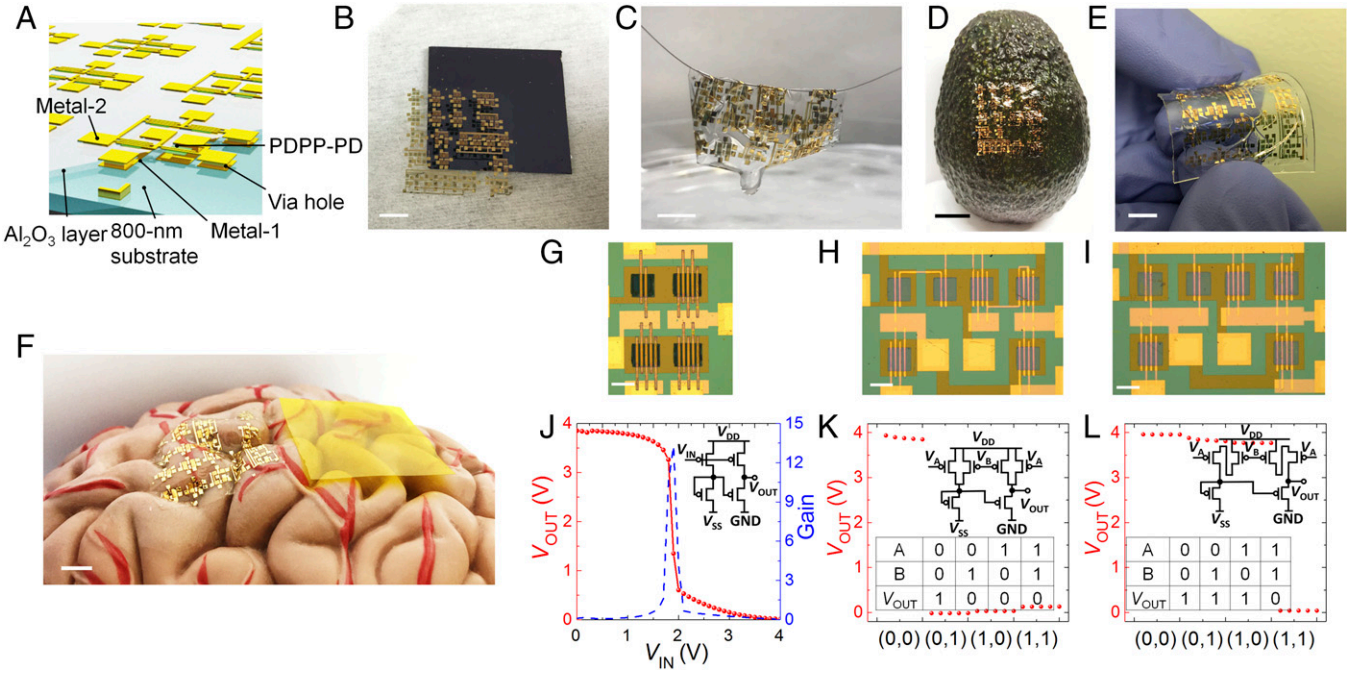

Fig. 4. Disintegrable pseudo-CMOS circuits based on PDPP-PD. (*A*) Device structures of the pseudo-CMOS circuits. (*B*) After dissolving the dextran layer, the device floated on water. (Scale bar: 5 mm.) (*C*) Device was picked up by a human hair. (Scale bar: 5 mm.) (*D*) Device was transferred onto the rough surface of an avocado. (Scale bar: 10 mm.) (*E*) Device transferred onto a PDMS substrate for electrical measurement. (Scale bar: 5 mm.) (*F*) Device was transferred onto a human brain model. (Scale bar: 5 mm.) (*G–L*) Optical microscopic images, circuit diagrams, and input–output characteristics for different logic gates. (Scale bar: 500 μm.) *G* and *J*, Inverter. *H* and *K*, NOR gate. *I* and *L*, NAND gate. V_{DD} = +4 V, V_{SS} = −4 V.

interconnects, and 25-nm ALD Al_2O_3 was used as the dielectric layer. The ALD-deposited Al_2O_3 can be decomposed in the pH 4.6 buffer solution with a rate of 1.5 nm/d (*SI Appendix*, Fig. S14). After self-assembled monolayer (SAM) modification, PDPP-PD can be directly spin-coated and patterned on the substrate using a fluoropolymer-protected oxygen plasma etching technique (*Materials and Methods*). Gold electrodes were deposited to form a top-contact configuration to complete the device. All of the fabrication processes, including spin-coating, photolithography, evaporation, and etching, were handled on rigid substrates. These processes are scalable to large device sizes. The device was then immersed in water to dissolve the dextran layer and release the ultrathin device (Fig. 4*B*). Fig. 4*C* shows that the device membrane can be picked up by a human hair. Furthermore, the device can be transferred onto any target substrate. For example, the thin device conforms well on a rough surface (Fig. 4*D*). For bio-integrated electronics, highly conformal coverage decreases the spacing between sensor devices and tissues with wrinkled surfaces, for example, the gyri and sulci of the brain, and therefore provides better recording of signals (38). Fig. 4*F* compares our device with a 25-μm polyimide (PI) substrate on a human brain model. PI films, 25 μm or thicker, are often used as the substrate for flexible electronics (39, 40). Our device showed much better conformal coverage, suggesting its potential applications in biointegrated electronics. The ultrathin transistor-covered sheet was transferred onto a polydimethylsiloxane (PDMS) or PI substrate to test their flexibility against bending at different radii of curvature (*SI Appendix*, Fig. S16). We observed less than a 5% change in the transfer characteristics of the devices before and after bending. As shown in Fig. 4 *B* and *J*, the PDPP-PD based pseudo-D inverter showed almost rail-to-rail output (i.e., output voltages close to the supply voltages, 4 or 0 V) with a sharp switching at V_{DD} = 1.9 V, very close to one-half of V_{DD} (2 V). The flexible inverter showed a large noise margin of 1.2 V (60% of the 1/2 V_{DD}; *SI Appendix*, Fig. S17), comparable to the state-of-the-art organic and carbon nanotube-based flexible logic circuits (41, 42). NOR and NAND gates consisting of six transistors were also fabricated using the pseudo-CMOS design. The input voltages, V_A and V_B, were set to be 4 or 0 V to represent logic "1" and "0," respectively (Fig. 4 *K* and *L*). Both NOR and NAND showed almost rail-to-rail voltage swings from 0 to 4 V, suggesting the potential of using these logic gates to construct more complex logic circuits. Although some traditional processes, such as lithography and vapor deposition, were included in the fabrication of the disintegrable circuits, we envision that these traditional processes can be replaced by other low-cost solution processes through further material optimization and process engineering (43, 44).

Totally Disintegrable Electronics

To date, almost all of the organic disintegrable electronics are fabricated using gold as the electrodes (4, 45). Although gold is a biocompatible material and has been widely used in implantable electronics (12, 38), it is not dissolvable and cannot "physically disintegrate" (46). To achieve completely disintegrable "transient" electronics, we investigated iron as the gate and source-drain electrodes for the polymer (Fig. 5*A*), because the work function of iron (4.8 eV) is close to the HOMO level of the polymer (5.11 eV). Fig. 5*B* shows the transfer characteristics of the iron devices. Compared with gold electrodes (work function: 5.1 eV), devices with iron electrodes showed a more negative threshold voltage, largely due to the mismatch between iron work function and the polymer HOMO level. However, the iron-based devices still showed reasonable hole mobilities of 0.12 ± 0.04 $cm^2/V{\cdot}s$ with on/off ratios $>10^4$ (*SI Appendix*, Fig. S18). We observed that our prepared devices are highly stable for several days in DI water (*SI Appendix*, Fig. S19) but can be rapidly degraded in a pH 4.6 buffer solution (containing 1 mg/mL cellulase). Fig. 5*C* displays the degradation process of our flexible devices. Specifically, we observed that the iron electrodes degrade rapidly under this condition, typically within 1 h (*SI Appendix*, Fig. S20). Other materials, including the conjugated polymers, cellulose substrate, and alumina, are all observed to be completely degraded within 30 d. For practical applications, the degradation speed of the device can be potentially controlled using appropriate decomposable encapsulation materials (*SI Appendix*, Fig. S21).

For reference, compared with the pH 4.6 buffer solution used for the complete dissolution of the devices, common fermented vinegar contains 5–20% acetic acid and has a pH of 2–3, and the pH of gastric acid in the human stomach is about 1.5–3.5. Thus, pH 4.6 or lower is a condition that exists in many biological processes. After disposing these electronics, they are likely to decompose under acidic biological conditions with little influence on our environment. Our ultrathin device is extremely lightweight at only 0.19 mg/cm^2 (*SI Appendix*, Table S1) or 1.9 g/m^2, which makes it among the lightest electronic devices reported to date (7, 18, 19, 26). For comparison, our device is about 40 times lighter than a sheet of typical office paper (80 g/m^2). The ingredients that might be potential hazards in the decomposed device are aluminum (5.9 $\mu g/cm^2$) and *p*-phenylenediamine (PPD) (0.48 $\mu g/cm^2$) (*SI Appendix*, Table S1). Based on published toxicity data, the aluminum content in our 1-cm^2 device is no greater than that in 100 mL of regular drinking water, and PPD is permitted by the US Food and Drug Administration for use as a hair dye. The 50% lethal dose (LD_{50}) of PPD is 80 mg/kg for rats, corresponding to 5.6 g for a 70-kg human. This is over 10^7 times higher than the maximum PPD concentration (0.48 $\mu g/cm^2$) in our device. Toxicity data for the decomposed product of DPP-CHO are not available; however, DPP derivatives are widely used as pigments in industrial coatings, printing inks, and tattoos. Toxicity studies showed that short-term inhalation of DPP pigments (6 h/d on 5 consecutive days) at high doses (30 mg/m^3) only caused minor effects on animal lungs (*SI Appendix*, Table S1). No expected ecological or toxicological threats to either human health or the environment were observed for DPP dyes used for tattoos. Moreover, compared with these commercial applications, the DPP concentration in our device is extremely low (3.92 $\mu g/cm^2$). Therefore, our devices

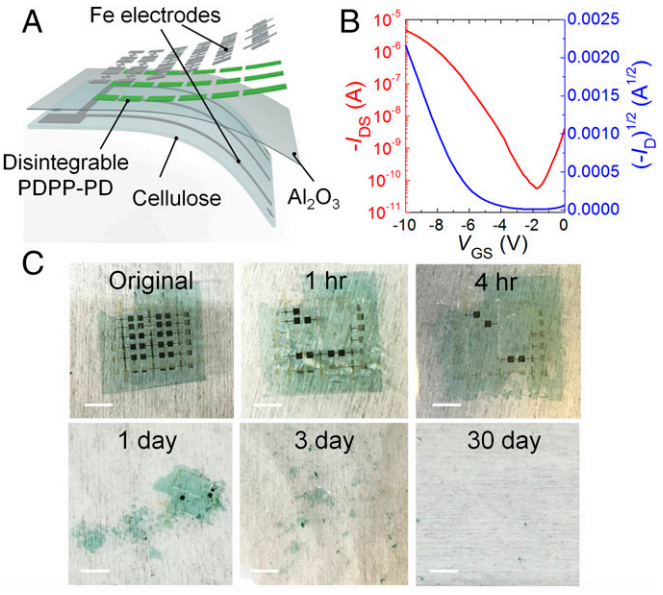

Fig. 5. Totally disintegrable electronics using iron as electrodes. (*A*) Schematic of the materials and device structure used for totally disintegrable electronics. (*B*) Transfer characteristic using Fe as the gate and source-drain electrodes. V_{DS} = −10 V. (*C*) Photographs of a device at various stages of disintegration. (Scale bars: 5 mm.)

are unlikely to present any potential hazards to either environment or human body.

In summary, we have demonstrated a fully decomposable and biocompatible semiconducting polymer and totally disintegrable flexible circuits. We showed that, using reversible imine chemistry, a completely decomposable conjugated polymer with high charge carrier mobility for various logic circuits is achievable and has electrical performance and solution processability comparable to traditional conjugated polymers. We further report a highly chemically and thermally stable ultrathin cellulose film as an optimized biodegradable substrate for transient and biodegradable electronics. Lastly, we prepare ultralightweight pseudo-CMOS logic circuits and totally disintegrable polymer transient electronics. Our described advances provide unique capabilities and broader applications for environmentally friendly and biointegrated organic electronics.

Materials and Methods

Materials. Detailed synthesis of the decomposable polymer can be found in *SI Appendix*.

Fabrication of the Ultrathin Disintegrable Logic Circuits. On the cellulose substrate, patterned gate electrodes consisting of 2.5-nm Ti/35-nm Au/2.5-nm Ti were thermally evaporated onto the cellulose substrate through a shadow mask. The first Ti layer was used for adhesion and the top Ti layer was used to provide nucleation sites for a 25-nm layer of Al_2O_3, which was deposited by ALD at 150 °C. The measured specific capacitance for the 25-nm Al_2O_3 is 280 nF/cm^2, slightly less than theoretical value of 301 nF/cm^2 (dielectric constant: 8.5). Vertical interconnect access holes were defined by photolithography using S1813 as photoresist and etched by an aluminum etchant for about 2 min. Interconnects (without source-drain electrodes) were patterned by thermal evaporation of 2-nm Ti/40-nm Au through a shadow mask. Before polymer deposition, the Al_2O_3 layer was modified with butylphosphonic acid as the SAM layer by spin-coating 2 mM butylphosphonic acid in trichloroethylene (TCE) at 3,000 rpm (Laurell, Model WS-650-23B) for 30 s and annealing at 100 °C for 10 min. A thin film of the polymer was deposited on the treated substrate by spin-coating PDPP-PD solution (5 mg/mL in TCE) at 1,000 rpm (Laurell, Model WS-650-23B) for 60 s, followed by thermal annealing at 150 °C under nitrogen.

To pattern the polymer semiconducting layer, a fluoropolymer-protected dry etching process was performed as follows. A 400-nm-thick PTFE AF 2400 (poly[4,5-difluoro-2,2-bis(trifluoromethyl)-1,3-dioxole-cotetrafluoroethylene]) was spin-coated on the PDPP-PD layer. In addition, an 80-nm-thick copper layer was thermally evaporated through a shadow mask to define the semiconducting layer. Oxygen plasma (150 W for 2 min) was used to etch away the PDPP-PD layer where the copper layer was not covered. The copper layer was then etched away by copper etchant (sodium persulfate). The PTFE AF 2400 was removed by soaking in fluorinated solvent (methoxyperfluorobutane) for 5 min. After the polymer layer was patterned, 40-nm gold was then deposited as the source and drain contacts using a shadow mask. To facilitate the dextran dissolution, the chip border was mechanically scratched. After the dextran was fully dissolved, the ultrathin device can be released and floated onto water. The device can be picked up and transferred to a target substrate (e.g., PDMS or polyimide film). All of the devices were tested under ambient conditions.

ACKNOWLEDGMENTS. This work was supported by Air Force Office for Scientific Research Grant FA9550-15-1-0106. It was partially supported by BASF. R.P. acknowledges support from Marie Curie Cofund, Beatriu de Pinós Fellowship AGAUR 2014 BP-A 00094. L. Shaw gratefully thanks the Kodak Graduate Fellowship for their support. Use of the Stanford Synchrotron Radiation Lightsource, SLAC National Accelerator Laboratory, was supported by the US Department of Energy, Office of Science, Office of Basic Energy Sciences under Contract DE-AC02-76SF00515.

1. Petti L, et al. (2016) Metal oxide semiconductor thin-film transistors for flexible electronics. *Appl Phys Rev* 3:021303.
2. Hwang S-W, et al. (2014) 25th anniversary article: Materials for high-performance biodegradable semiconductor devices. *Adv Mater* 26:1992–2000.
3. Hwang S-W, et al. (2012) A physically transient form of silicon electronics. *Science* 337:1640–1644.
4. Irimia-Vladu M (2014) "Green" electronics: Biodegradable and biocompatible materials and devices for sustainable future. *Chem Soc Rev* 43:588–610.
5. Bettinger CJ, Bao Z (2010) Organic thin-film transistors fabricated on resorbable biomaterial substrates. *Adv Mater* 22:651–655.
6. Loi MA, et al. (2005) Supramolecular organization in ultra-thin films of α-sexithiophene on silicon dioxide. *Nat Mater* 4:81–85.
7. Kaltenbrunner M, et al. (2013) An ultra-lightweight design for imperceptible plastic electronics. *Nature* 499:458–463.
8. Sekitani T, et al. (2009) Stretchable active-matrix organic light-emitting diode display using printable elastic conductors. *Nat Mater* 8:494–499.
9. Tee BCK, et al. (2015) A skin-inspired organic digital mechanoreceptor. *Science* 350:313–316.
10. Henson ZB, Müllen K, Bazan GC (2012) Design strategies for organic semiconductors beyond the molecular formula. *Nat Chem* 4:699–704.
11. Klauk H, Zschieschang U, Pflaum J, Halik M (2007) Ultralow-power organic complementary circuits. *Nature* 445:745–748.
12. Irimia-Vladu M, et al. (2010) Biocompatible and biodegradable materials for organic field-effect transistors. *Adv Funct Mater* 20:4069–4076.
13. Irimia-Vladu M, et al. (2012) Indigo—a natural pigment for high performance ambipolar organic field effect transistors and circuits. *Adv Mater* 24:375–380.
14. Oh JY, et al. (2016) Intrinsically stretchable and healable semiconducting polymer for organic transistors. *Nature* 539:411–415.
15. Nielsen CB, Turbiez M, McCulloch I (2013) Recent advances in the development of semiconducting DPP-containing polymers for transistor applications. *Adv Mater* 25:1859–1880.
16. Lei T, Wang J-Y, Pei J (2014) Design, synthesis, and structure-property relationships of isoindigo-based conjugated polymers. *Acc Chem Res* 47:1117–1126.
17. Khodagholy D, et al. (2013) In vivo recordings of brain activity using organic transistors. *Nat Commun* 4:1575.
18. White MS, et al. (2013) Ultrathin, highly flexible and stretchable PLEDs. *Nat Photonics* 7:811–816.
19. Kaltenbrunner M, et al. (2012) Ultrathin and lightweight organic solar cells with high flexibility. *Nat Commun* 3:770.
20. Yang C-J, Jenekhe SA (1995) Conjugated aromatic polyimines. 2. Synthesis, structure, and properties of new aromatic polyazomethines. *Macromolecules* 28:1180–1196.
21. Belowich ME, Stoddart JF (2012) Dynamic imine chemistry. *Chem Soc Rev* 41:2003–2024.
22. Hu B, et al. (2012) A multilevel memory based on proton-doped polyazomethine with an excellent uniformity in resistive switching. *J Am Chem Soc* 134:17408–17411.
23. Holst JR, Trewin A, Cooper AI (2010) Porous organic molecules. *Nat Chem* 2:915–920.
24. Chortos A, Liu J, Bao Z (2016) Pursuing prosthetic electronic skin. *Nat Mater* 15:937–950.
25. Xie C, Lin Z, Hanson L, Cui Y, Cui B (2012) Intracellular recording of action potentials by nanopillar electroporation. *Nat Nanotechnol* 7:185–190.
26. Salvatore GA, et al. (2014) Wafer-scale design of lightweight and transparent electronics that wraps around hairs. *Nat Commun* 5:2982.
27. Yu KJ, et al. (2016) Bioresorbable silicon electronics for transient spatiotemporal mapping of electrical activity from the cerebral cortex. *Nat Mater* 15:782–791.
28. Zhu H, Fang Z, Preston C, Li Y, Hu L (2014) Transparent paper: Fabrications, properties, and device applications. *Energy Environ Sci* 7:269–287.
29. Jung YH, et al. (2015) High-performance green flexible electronics based on biodegradable cellulose nanofibril paper. *Nat Commun* 6:7170.
30. Zhu H, et al. (2013) Biodegradable transparent substrates for flexible organic-light-emitting diodes. *Energy Environ Sci* 6:2105–2111.
31. McCormick CL, Callais PA, Hutchinson BH (1985) Solution studies of cellulose in lithium chloride and *N,N*-dimethylacetamide. *Macromolecules* 18:2394–2401.
32. Kontturi E, Thüne PC, Niemantsverdriet JW (2003) Novel method for preparing cellulose model surfaces by spin coating. *Polymer (Guildf)* 44:3621–3625.
33. McCulloch I, Salleo A, Chabinyc M (2016) ORGANIC DEVICES. Avoid the kinks when measuring mobility. *Science* 352:1521–1522.
34. Mei J, Kim DH, Ayzner AL, Toney MF, Bao Z (2011) Siloxane-terminated solubilizing side chains: Bringing conjugated polymer backbones closer and boosting hole mobilities in thin-film transistors. *J Am Chem Soc* 133:20130–20133.
35. Huang TC, et al. (2011) Pseudo-CMOS: A design style for low-cost and robust flexible electronics. *IEEE Trans Electron Dev* 58:141–150.
36. Sekitani T, et al. (2016) Ultraflexible organic amplifier with biocompatible gel electrodes. *Nat Commun* 7:11425.
37. Myny K, Steudel S (2016) Flexible thin-film NFC transponder chip exhibiting data rates compatible to ISO NFC standards using self-aligned metal-oxide TFTs. *2016 IEEE International Solid-State Circuits Conference (ISSCC)* (IEEE, Piscataway, NJ), pp 298–299.
38. Kim D-H, et al. (2010) Dissolvable films of silk fibroin for ultrathin conformal biointegrated electronics. *Nat Mater* 9:511–517.
39. Chen H, Cao Y, Zhang J, Zhou C (2014) Large-scale complementary macroelectronics using hybrid integration of carbon nanotubes and IGZO thin-film transistors. *Nat Commun* 5:4097.
40. Wang C, et al. (2013) User-interactive electronic skin for instantaneous pressure visualization. *Nat Mater* 12:899–904.
41. Wang H, et al. (2014) Tuning the threshold voltage of carbon nanotube transistors by n-type molecular doping for robust and flexible complementary circuits. *Proc Natl Acad Sci USA* 111:4776–4781.
42. Gelinck G, Heremans P, Nomoto K, Anthopoulos TD (2010) Organic transistors in optical displays and microelectronic applications. *Adv Mater* 22:3778–3798.
43. Yan H, et al. (2009) A high-mobility electron-transporting polymer for printed transistors. *Nature* 457:679–686.
44. Sirringhaus H, et al. (2000) High-resolution inkjet printing of all-polymer transistor circuits. *Science* 290:2123–2126.
45. Irimia-Vladu M, Głowacki ED, Voss G, Bauer S, Sariciftci NS (2012) Green and biodegradable electronics. *Mater Today* 15:340–346.
46. Yin L, et al. (2014) Dissolvable metals for transient electronics. *Adv Funct Mater* 24:645–658.